Theme 02-1-1086-2009/2023

Strangeness in nucleon and nuclei

The HyperNIS + SRC project

V. D. Aksinenko, T. Atovullaev, A. Atovullaeva, A. V. Averyanov, A. E. Baskakov, S. N. Bazylev, A. G. Bochkova, V. F. Chumakov, D. V. Dementiyev, A. A. Fechtchenko, A. A. Fedyunin, I. A. Filippov, S. V. Gertsenberger, A. S. Khvorostukhin, A. M. Korotkova, D. O. Krivenkov, R. I. Kukushkina, V. V. Lenivenko, J. Lukstins, S. M. Nepochatykh, O. V. Okhrimenko, A. N. Parfenov, N. G. Parfenova, M. A. Patsyuk, S. N. Plyashkevich, P. A. Rukoyatkin, A. V. Salamatin, A. Sheremetiev, A. V. Shipunov, M. Shitenkov, A. V. Shutov, I. V. Slepnev, V. M. Slepnev, E. A. Strokovsky, A. L. Voronin
VBLHEP JINR
S. V. Tereschenko, V. V. Tereschenko
DLNP JINR
P. I. Kharlamov, M. G. Korolev, M. M. Merkin
SINP Lomonosov Moscow State University,
T. Nakano, A. Tokiyasu
RCNP, Osaka University Japan,
E. Piasetzky, G. Johansson
Tel-Aviv University Israel,
O. Hen, J. Kalbow
Massachusetts Institute of Technology USA

Project leaders D.Krivenkov, J.Lukstins, M.Patsyuk

Abstract

The experimental program of the joined HyperNIS + SRC project consists of two sections: HyperNIS and SRC.

The HyperNIS program is aimed at investigation of the role which strangeness plays in nuclei, namely open strangeness in hypernuclei, and in nucleon where the talk is about correlated $\bar{s}s$ pairs, i.e., hidden intrinsic strangeness. In its turn the HyperNIS program consists of two parts which can be realized with the HyperNIS spectrometer. Taking into account the spectrometer capacity our efforts are concentrated on hypernuclear research. The goal of the first part of the program is the study of the lightest neutron-rich hypernuclei. In particular, it is necessary to establish firmly if the hypernucleus ${}^{6}_{\Lambda}$H really exists. It should be noted that in the same experiment the lifetimes and production cross sections of ${}^{4}_{\Lambda}$H and ${}^{3}_{\Lambda}$H will be investigated. The further experiment will be the study of ${}^{6}_{\Lambda}$He, previously observed only in emulsion experiments. The next step of this program is aimed to determine the binding energy of the loosely bound ${}^{3}_{\Lambda}$H hypernucleus.

The properties of nuclei are determined by interactions of their constituents: nucleons on the level of the lower resolution and quarks and gluons at the high

resolution. The relation between these two descriptions remains a challenge. Short range correlated nucleon pairs which are temporary fluctuations of strongly interacting nucleons at a distance of around nucleon radius and with individual momenta larger than that of mean-field nucleons, are coupled to both nuclear scales. Electron scattering experiments have shown the far-reaching impacts of short range correlations (SRCs) have on the many-body systems, the nucleon-nucleon interaction, and the nucleon substructure.

The usage of ion beams opens completely new pathways in SRC research. Shooting a nuclear beam on a proton target makes possible to study properties of nuclear fragments after the quasi-elastic knockout of a single nucleon or SRC pair. The first SRC experiment at BM@N (2018) has shown that detection of an intact ^{11}B nucleus after an interaction makes the scattering happen on a transparent carbon nucleus. Initial- and final-state interactions are suppressed for the set of quasi-elastic knockout events with ^{11}B in the final state. Also, 23 events of SRC-breakups showed agreement in SRC properties as known from electron beam experiments. The next stage of the SRC studies at BM@N (at 2022) included an improved setup with large hadron calorimeters for proton-pion separation, a better timing resolution with new scintillator trigger counters, and a laser system for simultaneous calibration of all scintillator detectors without the beam. The data analysis is ongoing.

The emphasis for the next SRC experiment planned at the new HyperNIS location will be refined basing on the analysis results. The main idea of this proposal is to show that the SRC setup can fit into the HyperNIS setup with a minimal distraction. However, a larger band of the magnetic field is needed to obtain the required resolution. For that a second magnet needs to be installed. This document intends to allow the start of the engineering work on the site necessary to fit there the second dipole magnet.

HyperNIS

1 Aims of the project

The project is aimed to study the lightest neutron-rich hypernuclei; in particular, to search for and to study properties of ${}^{6}_{\Lambda}$H. Simultaneously, lifetimes and production cross sections of ${}^{4}_{\Lambda}$H and ${}^{3}_{\Lambda}$H will be studied in the same experiment because we will use reaction

$$^{7}\mathrm{Li} + \mathrm{C} \rightarrow {}^{\mathrm{A}}_{\Lambda}\mathrm{H} + \mathrm{K} + \mathrm{p(d,t,n)} + \ldots \rightarrow {}^{\mathrm{A}}\mathrm{He} + \pi^{-} + \ldots, \quad (1)$$

where A = 3, 4, 6. Moreover, production and observation of ${}^{4}_{\Lambda}$H and ${}^{3}_{\Lambda}$H hypernuclei are the precise reference signal to make sure that ${}^{6}_{\Lambda}$H should be seen in the same run if it exists or that there are no stable forms of ${}^{6}_{\Lambda}$H if the last will not be observed. This task is regarded as the very first experiment because at Frascati experiment [1, 2, 3] evidence of only three events was reported and controversial data were obtained at J-PARC [4], where no signal was detected instead of expected 50 events. On the other hand, before the J-PARC experiment A. Gal predicted that the possibility to see the ${}^{6}_{\Lambda}$H signal, is low in that case. A reason is that the spectrometer at J-PARC is not suited well for the task since the energy of recoil nuclei is too high while the pion beam produces hypernuclei of high excitation levels that is impossible in the case of low hypernucleus binding energy. Moreover, to produce ${}^{6}_{\Lambda}$H using ^{6}Li target, the double charge exchange reaction is necessary. The process is suppressed and a lot of uncertainties should be solved to predict the production rate. Anyway, the search of ${}^{6}_{\Lambda}$H was not a part of J-PARC research program for the period till 2030.

The result of the ${}^{6}_{\Lambda}$H hypernucleus search should be a turning point of our program. If the ${}^{6}_{\Lambda}$H production cross section is high enough and the event yield is large, one should choose between two ways: either to continue the study of ${}^{6}_{\Lambda}$H properties or to search for the ${}^{8}_{\Lambda}$H hypernucleus. It seems that the search of and the possible discovery of the ${}^{8}_{\Lambda}$H hypernucleus will be the best decision. Particularly, since it is a very difficult task to investigate ${}^{8}_{\Lambda}$H using pion or kaon beams. The results of these two experiments will determine if it is better to study properties of the new hypernuclei or to turn to the ${}^{6}_{\Lambda}$He and ${}^{3}_{\Lambda}$H hypernucleus program.

The second way is also very rewarding. The study of the poorly investigated hypernucleus ${}^{6}_{\Lambda}$He will be a natural continuation of lithium beam experiments. With carbon beams, the program can be extended to determine the effective Hamiltonian of the ΛN$\rightarrow$NN weak interaction.

One more original and attractive idea is the experimental estimation of the binding energy of the loosely bound ${}^{3}_{\Lambda}$H hypernucleus. Here the approach suggested in the Laboratory of High Energies (JINR, Dubna) will be used. In this approach the hypernuclei under study are being produced by an excitation of the beam nuclei and the hypernuclei decay is being observed at a distance of tens of centimeters behind the production

target. Thus, the passage of the hypernuclei "beam" through materials with different nuclear charges, Z, can be investigated in order to obtain an experimental estimation of the ${}^{3}_{\Lambda}$H binding energy. However, the best source of the ${}^{3}_{\Lambda}$H beam is the primary ^{4}He beam.

2 Introduction and physics motivation

The Hypernuclear program at Dubna [5, 6] was started in 1988 with the setup based on 2-m streamer chamber. The investigation of the light hypernuclei production and decay [6] was done, namely, the lifetime of ${}^{4}_{\Lambda}$H and ${}^{3}_{\Lambda}$H as well as their production cross sections were measured. It was shown that the approach in which the momentum of hypernuclei produced in the beams of relativistic ions is close to the momentum of the projectiles, was quite effective for measurements of hypernuclei lifetimes and production cross sections. The dedicated and very selective trigger on two body hypernuclei decays with negative pion was the key point of this approach. As a result, the accuracy of lifetime measurements was, therefore, restricted mainly by statistical errors. The values of the experimental cross section were in good agreement with the results of the calculations [7] (see also the review [8]) performed using the coalescence model. It should be noted that hypernucleus lifetime up to now remains an actual problem.

High energy collisions like ALICE experiment at CERN provides significant statistic of ${}^{3}_{\Lambda}$H hypernuclei (and antinuclei as well) produced by coalescence effects. While results presented at the Conferences Hyp2015 and Hyp2018 were controversial (see below) and triggered new experiments, in Prague Hyp2022 Alice and STAR experiments presented quite similar lifetime results for hypernucleus ${}^{3}_{\Lambda}$H but binding energy presented by ALICE was a surprise. Most of the earlier measurements [9, 10, 11] presented at Hyp2015 have shown ${}^{3}_{\Lambda}$H lifetime values of $140 - 200$ ps (155 ps at STAR, 181 ps at ALICE) while theory predicts $240 - 260$ ps (256 ps by H. Kamada [12], 233-244 ps by T. Motoba [13]). Different measurements and predictions are collected in Fig. 1. At the next conference, Hyp2018, controversial ${}^{3}_{\Lambda}$H lifetime results were reported by ALICE $\tau = 223^{+41}_{-33}(\text{stat.})\pm 20(\text{syst.})$ ps [14] and by STAR $\tau = 142^{+24}_{-21}(\text{stat.}) \pm 29(\text{syst.})$ ps [15], see Fig. 2. ${}^{3}_{\Lambda}$H measured lifetime values in 2022, $253\pm 11(\text{stat.})\pm 6(\text{syst.})$ ps by ALICE [16] and $221\pm 15(\text{stat.})\pm 19(\text{syst.})$ ps by STAR [17], are coincided to each other.

In all previous hypernuclear experiments except the above mentioned Dubna experiments [18] and the Heavy Ion Beam experiment at GSI, Darmstadt [19, 20], hypernuclei are produced in various processes of a target excitation. The common feature of all such experiments is that momentum of the produced hypernucleus is low and the last decays practically at the production point inside the target. On the contrary, in Dubna experiments, the energy of hypernuclei is only slightly lower than that of the beam nuclei, see Fig. 3. Therefore, the hypernucleus lifetime in the laboratory reference frame is increased by the Lorentz factor $3 - 7$ and a significant part of hypernuclei decays far behind the production target. Thus, the location of the decay vertices can be used for identification of a hypernucleus decay and for determination of the lifetime of the observed hypernuclei by measurements of their decay path distribution. In other words,

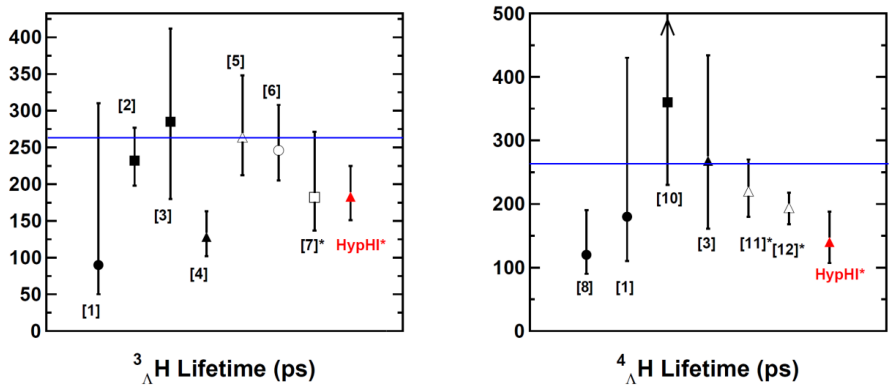

Figure 1: World data comparison of ${}^{3}_{\Lambda}$H and ${}^{4}_{\Lambda}$H lifetimes presented by Rappold in Proceedings [11] where references are listed. It should be said that ${}^{4}_{\Lambda}$H lifetime value noted as [11] is result of our previous experiment [21]. Values obtained in the HypHI experiment [11], are indicated as "HypHI". The horizontal line at 263.2 ps shows the known lifetime of the Λ hyperon. References to counter experiments are marked by an asterisk.

the lifetime "is converted" into the flight path which could be unambiguously measured with a good accuracy.

The HyperNIS program is focused on properties of hypernuclei with a neutron rich halo. In the last time, properties of neutron rich hypernuclei and double hypernuclei are highly anticipated to revise the theory of neutron stars to solve the hyperon puzzle. The distribution of the baryon chemical potential in neutron stars predicts that a part of baryons should be Lambda particles but inclusion of Lambdas can change most of temporary suggestions for the equation of state (EoS) so that $1.4 - 1.5$ solar masses would be a limit of the neutron star mass while it is known that masses of two of them are equal to two solar masses [22]. Recently, the theory suggests how to solve the problem [23] but new hypernuclear experimental data will help to choose the proper way.

First of all, the study of ${}^{6}_{\Lambda}$H hypernucleus will be carried out with the ^{7}Li beam:

$$^{7}\mathrm{Li} + C \rightarrow {}^{A}_{\Lambda}\mathrm{H} + \mathrm{p(d,t,n)} + \ldots \rightarrow {}^{A}\mathrm{He} + \pi^{-} + \ldots \quad \text{where A=3, 4, 6.} \qquad (2)$$

We have chosen the ^{7}Li beam because an extra proton from ^{7}Li can be stripped by fragmentation while an additional charge exchange reaction is necessary if the ^{6}Li beam is used to produce the ${}^{6}_{\Lambda}$H hypernucleus. The probability of fragmentation is much higher than that of the charge exchange reaction. The double charge exchange problem considering ${}^{6}_{\Lambda}$H hypernucleus production is discussed, for example, by A. Sakaguchi [24].

An evidence for three ${}^{6}_{\Lambda}$H hypernuclei was reported from Frascati [1, 2]. In the concluding remarks at the closing of the 11th International Conference on Hypernuclei and Strange Particle Physics held in 2012 in Barcelona, the first observation of ${}^{6}_{\Lambda}$H was mentioned by T. Nagae [25] as one of the four main achievements in hypernuclear physics reached during the last years. On the other hand, E10 collaboration at the J-PARC experiment did not observe the missing mass peak corresponding to ${}^{6}_{\Lambda}$H production [4, 24]. However, before the start of the E10 experiment, A. Gal noted at Barcelona conference that there will be a low probability to see the signal from ${}^{6}_{\Lambda}$H at

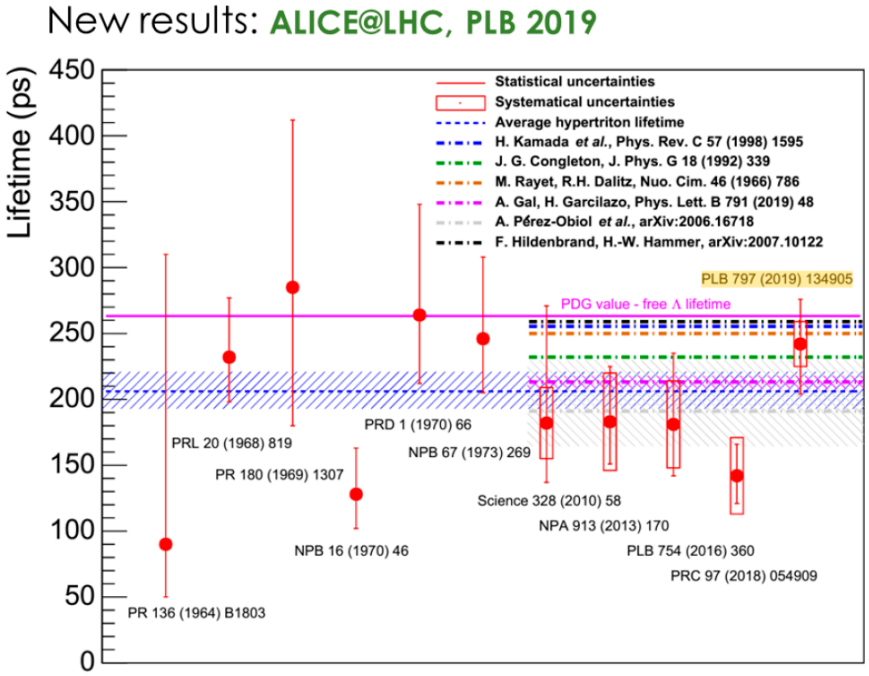

Figure 2: The summary of hypertritium lifetime measurement value in the period from 1964 till 2022. The data are taken from A. Ramos presentation at Hyp2022 in Prague [14].

the J-PARC experiment due to the high transferred momentum and, consequently, the high momentum and excitation of produced hypernuclei. Theoretical predictions are strongly model dependent and controversial as well. For example, E. Hiyama and others [26] have calculated that ${}^{6}_{\Lambda}$H is not a stable nucleus and should decay into ${}^{4}_{\Lambda}$H+n+n if one takes into account the parameters of ^{5}H resonance measured up to now. At the same time there are estimates [27, 28] showing that the binding energy of ${}^{6}_{\Lambda}$H should be about a few MeV. So, it is necessary to carry out an experiment that can test existence of ${}^{6}_{\Lambda}$H hypernucleus without a doubt.

At J-PARC, the search of ${}^{6}_{\Lambda}$H was the first phase of the E10 experiment which was performed at the J-PARC 50 GeV proton-synchrotron facility. However, the search of ${}^{6}_{\Lambda}$H using the ^{6}Li(π^-,K$^+$) reaction at the pion beam momentum of 1.2 GeV/c gave no events again [24]. Considering the theory A. Sakaguchi [24] should be cited at Sendai Conference:

"The results of the theoretical calculations indicate that the binding energy of ${}^{6}_{\Lambda}$H is sensitive to the interactions and the models employed in the calculations and also the structure of the ^{5}H nucleus. The FINUDA collaboration also made another assignment of the 3 candidate events in which the 3 events of ${}^{6}_{\Lambda}$H corresponded to different states as shown in the most right part in Fig. 3 (we present this Figure from Sakaguchi paper as Fig. 4). The level structure of ${}^{6}_{\Lambda}$H still has ambiguities only with the FINUDA result, and complementary measurements are necessary (we emphasize this statement). The production mechanism by the DCX (double charge exchange) reaction and the struc-

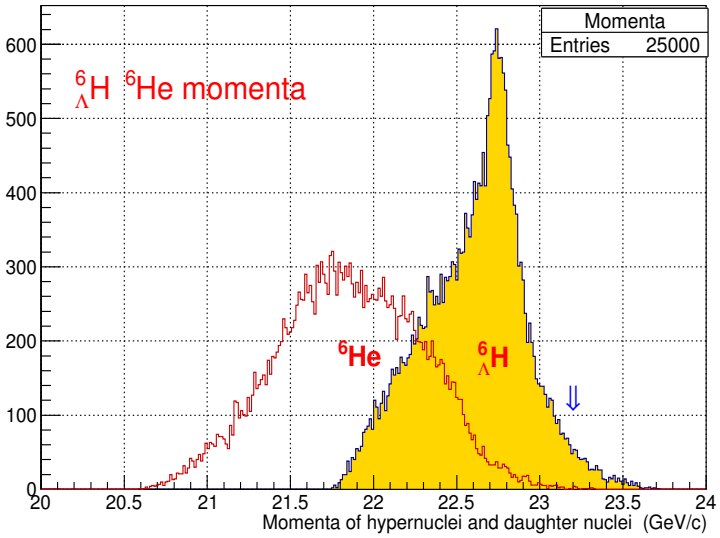

Figure 3: Expected distributions of momenta of $^{6}_{\Lambda}$H hypernuclei and the daughter nuclei, ^{6}He, are shown. The beam momentum, 23.2 GeV/c, is indicated by the arrow. Due to Fermi motion and beam fragmentation, momenta of few hypernuclei are higher than the mean momentum value for 6 nucleons (^{7}Li beam).

ture of the neutron-rich $^{6}_{\Lambda}$H hypernuclei are not well understood, yet. More detailed analysis of the already obtained experimental data and further experimental studies of other neutron-rich $^{6}_{\Lambda}$H hypernuclei are necessary."

Anyway, it seems that if pion beams are used, the $^{6}_{\Lambda}$H production cross section is tiny and more precise experiments will be difficult. On contrary, we suggest to use ^{7}Li fragmentation due to a much higher reaction probability instead of DCX for ^{6}Li.

At this point one should note that no hypernuclei were directly observed at Frascati and J-PARC experiments. Only secondary effects like negative pions assumed to be products of the $^{6}_{\Lambda}$H decay or the missing mass of the possible production reaction, were determined. Since statistics at Frascati was very low (only 3 candidates) and no signal at J-PARC was observed, the situation is controversial. Therefore, a crucial experiment can be carried out at the VBLHEP of JINR. The search of $^{6}_{\Lambda}$H with the HyperNIS spectrometer to obtain quite high statistics (few hundreds of detected events), should be made in order to measure the lifetime and production cross sections. That will provide a basis to solve the problem whether hyperons indeed are acting as a "glue" in the vicinity of the neutron rich drip line. Also, the mass of the isotope $^{6}_{\Lambda}$H can be measured with the use of our magnetic spectrometer.

Actually, at the Dubna experiment, three isotopes of hydrogen hypernuclei ($^{3}_{\Lambda}$H, $^{4}_{\Lambda}$H, $^{6}_{\Lambda}$H) have to be produced simultaneously. It must be stressed that $^{3}_{\Lambda}$H and $^{4}_{\Lambda}$H can be used as "reference points" to confirm production and the decay of $^{6}_{\Lambda}$H. Sure, lifetimes of all these hypernuclear isotopes can be measured as well.

Production of hypernuclei with a large neutron excess and a neutron halo was discussed by L. Majling since 1994 [29, 30]. A possibility was pointed out to study the baryon-baryon interaction in the system with an extremely large value of $N/Z = 6$.

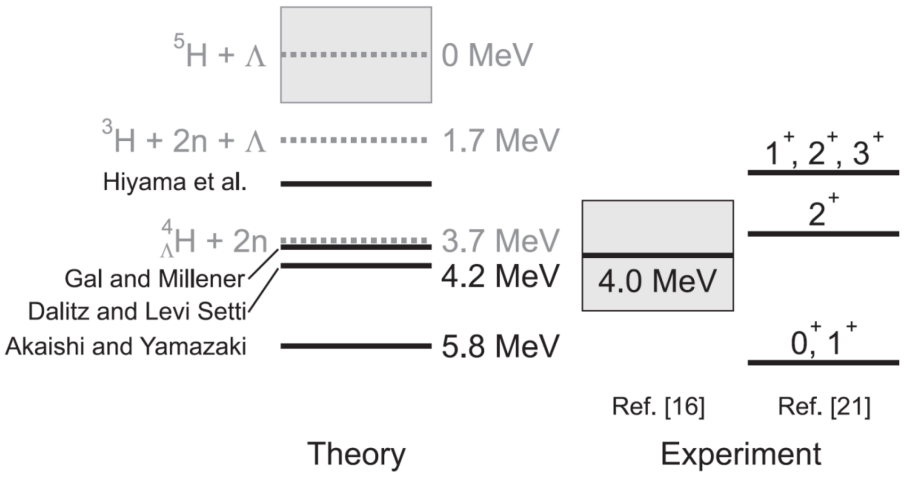

Figure 4: A summary of energy levels of $^6_Λ$H. In the left side theoretically calculated binding energies from [31, 32, 27, 26] are shown. The right side shows energy levels and binding energies reported by the FINUDA collaboration in [1, 2]. All the binding energies are measured from the ^{5}H+Λ threshold.

It was also emphasized that the measurement of the $^6_Λ$H mass allows verification of the assumption that the binding energy of neutron-rich hypernuclei increases due to the specific "coherent $Λ - Σ$ mixing mechanism" [33, 34]. It should be noted that there is a chain of four nuclei with two neutron halo and different compositions of the S-shell core: with and without Λ hyperon, namely the nuclei ^{5}H, $^6_Λ$H, ^{6}He, $^7_Λ$He. Thus, the study of $^6_Λ$H properties as well as those of $^6_Λ$He, will be significant for the theory. Also it was noted that existence of the $^8_Λ$H hypernucleus might be possible. If the first experiment with $^6_Λ$H will be successful, the following search of $^8_Λ$H hypernucleus is the most natural aim. We propose to use the ^{9}Li beam for such the experiment. Also let us note that the search for $^8_Λ$H using pion or kaon beams is even more difficult than the study of $^6_Λ$H. The ^{9}Li beam will be created as a secondary beam when carbon is accelerated one. The chain of possible processes is

$$^{12}\mathrm{C} + \mathrm{Al} \rightarrow ^9\mathrm{Li} + \mathrm{C} + \ldots, \quad ^9\mathrm{Li} \rightarrow ^8_Λ\mathrm{H} + \mathrm{p} \rightarrow ^8\mathrm{He} + \pi^- + \mathrm{p}.$$

Lifetimes of ^{9}Li and ^{8}He are of the order of hundred milliseconds that is long enough for the experiment.

Expected production cross sections of the lightest hypernuclei are given in Table 1. New data from the present project will significantly improve the description of the hypernucleus production process. Taking into account values from the table we have estimated the possible counting rate of $^4_Λ$H pionic decays equal to 600 events per day in the case of ideal Nuclotron operation conditions (the spill length is 5 s, there are no intensity pulsations, etc.). However, real tests have shown that this value should be reduced few times to $150 - 200$ events per day. Reasons are the spill duration is shorter and we used a lower beam intensity on the spectrometer since the intensity pulsation causes overlapping of two beam particles inside 50 ns time interval with overlapping

of signal amplitudes. Properties of the Nuclotron extracted beam are continuously improved but, at the moment, the value $150 - 200$ events per day is most realistic. If we suppose that the binding energy of ${}^{6}_{\Lambda}$H is low, we can expect that its production cross section is of the same order as for ${}^{3}_{\Lambda}$H. Then, one can expect to register $30 - 40$ events of ${}^{6}_{\Lambda}$H per day. But we should underline that all estimates are based on the idea that coalescence is similar in all hydrogen hypernuclei production processes.

Table 1: Measured and estimated cross sections of hypernucleus production. The calculations are taken from [7]. For the ^{7}Li beam on the carbon target, we have measured [35] the cross section of the charge change, $\sigma_{cc} = 650 \pm 20$ mb.

Beam	Hyper-	Energy,	Cross sec., μb	
	nuclei	AGeV	Theory	Exp.
^{3}He	${}^{3}_{\Lambda}$H	5.14	0.03	$0.05^{+0.05}_{-0.02}$
^{4}He	${}^{3}_{\Lambda}$H	3.7	0.06	< 0.1
	${}^{4}_{\Lambda}$H	2.2	0.08	< 0.08
		3.7	0.29	$0.4^{+0.4}_{-0.2}$
^{6}Li	${}^{3}_{\Lambda}$H	3.7	0.09	$0.2^{+0.3}_{-0.15}$
	${}^{4}_{\Lambda}$H	3.7	0.2	$0.3^{+0.3}_{-0.15}$
^{7}Li	${}^{7}_{\Lambda}$Li	3.0	0.11	< 1
	${}^{6}_{\Lambda}$He	3.0	0.25	< 0.5

At the next stage of the experiment, the ${}^{6}_{\Lambda}$He hypernucleus will be investigated with the ^{6}Li beam. ${}^{6}_{\Lambda}$He will be produced in peripheral interactions of lithium with the carbon target and the trigger will be tuned in order to select pionic decays producing the negative pion and the daughter lithium nucleus emitted from the decay region:

$$^6\mathrm{Li} + \mathrm{C} \rightarrow {}^{6}_{\Lambda}\mathrm{He} + \ldots \rightarrow {}^{6}\mathrm{Li} + \pi^- + \ldots \tag{3}$$

It was established that ${}^{6}_{\Lambda}$He hypernucleus is loosely bound (the neutron separation energy, $B = 0.17 \pm 0.10$ MeV). But its lifetime and production cross section were not measured up to now. The measurement of the ${}^{6}_{\Lambda}$He lifetime is the first task of the ${}^{6}_{\Lambda}$He experiment. While ${}^{5}_{\Lambda}$He hypernuclei are investigated very well, the study of ${}^{6}_{\Lambda}$He was stopped after emulsion experiments since it is not so easy to produce ${}^{6}_{\Lambda}$He hypernuclei in other experiments due to weakly bound neutron within it. Meanwhile, ${}^{5}_{\Lambda}$He is easily produced in kaon or pion beams if a ^{6}Li target is used.

The method of Coulomb dissociation suggested in [21, 36, 37, 38], will be exploited for the experimental estimation of ${}^{3}_{\Lambda}$H and ${}^{6}_{\Lambda}$He binding energies. This method is

interesting from the experimental point of view because interactions of hypernucleus "beam" should be investigated.

More complicated experimental skill and instruments should be used for the next stage of research tasks devoted to the study of nonmesonic decays of hypernuclei. It is well known that removing one neutron from ^{9}Be results in ^{8}Be* with the subsequent double α-decay. Due to this salient feature of the core of nuclei ^{9}Be and ^{9}B, it may be possible to identify final states of the residual nucleus. In the experiment, one should register a chain of decays, for example, $^{10}_{\Lambda}$B which decays as $^{10}_{\Lambda}\mathrm{B} \to n + p +\ ^8\mathrm{Be}^*$ with the subsequent ^{8}Be* decay emitting two α's within a very small angle. We are going to experimentally determine branching ratios $\Gamma^{n\,(p)}_{\alpha\alpha\,i}$ for exclusive decays of $^{10}_{\Lambda}$Be and $^{10}_{\Lambda}$B hypernuclei. This task can be made during SRC run at HyperNIS setup with the carbon beam.

The energy of the α-particles determines the final state of the residual nucleus ^{8}Be, i.e., its quantum numbers and hence also the actual weight of the four possible wave functions of the NΛ-pair: $p_{\frac{1}{2}}s_\Lambda$ with J = 0, 1 and $p_{\frac{3}{2}}s_\Lambda$ with J = 1, 2. The branching ratios $\Gamma^{n\,(p)}_{\alpha\alpha\,i}$ depend on various combinations of four matrix elements $w^{SJ}_{\ell\tau}$. As a result, their study offers a unique possibility for determination of all needed matrix elements of the weak interaction [18, 39]. The knowledge of these $w^{SJ}_{\ell\tau}$ will open a possibility to extend the phenomenological model of Block & Dalitz [40] up to p-shell hypernuclei.

Because the two alpha particles and the decay products of the excited hypernuclei are emitted in a very narrow cone, additional high resolution detectors should be installed to detect twin alpha particles. Calculations have shown that gas electron multiplier (GEM) detectors with the 10×10 cm^2 area can solve the problem. An additional trigger counter with a thin (1 mm) quartz radiator can suppress in 30-50 times the background coming from the beam nuclei fragmentation in the trigger detectors. Considering the spectrometer capability for such the experiment we analyze and test a possibility to install few high resolution trackers, namely scintillating fiber detectors, GEM, and microstrip detectors.

3 Spectrometer scheme

The configuration of the spectrometer is presented in Fig. 5. The carbon target is placed at 12 cm along the beam and has the cross section 3×3 cm^2 and the density 20.4 g/cm^2. When hyperhydrogen ($^3_{\Lambda}$H or $^4_{\Lambda}$H or $^6_{\Lambda}$H) is produced in interactions of the ^{7}Li beam nuclei with the carbon target, the pionic decay

$$^A_{\Lambda}\mathrm{H} \to {}^A\mathrm{He} + \pi^- \quad (A = 3, 4, 6) \tag{4}$$

will occur inside the vacuum vessel with a rather high probability. The Cherenkov and scintillation counters (the trigger detectors B and C, correspondingly) are tuned to measure the charge difference between hypernucleus and its decay products. Taking into account that the resolution of a Cherenkov counter is better than scintillation one, a block of four Cherenkov counters is used as B detector as discussed above. Blocks

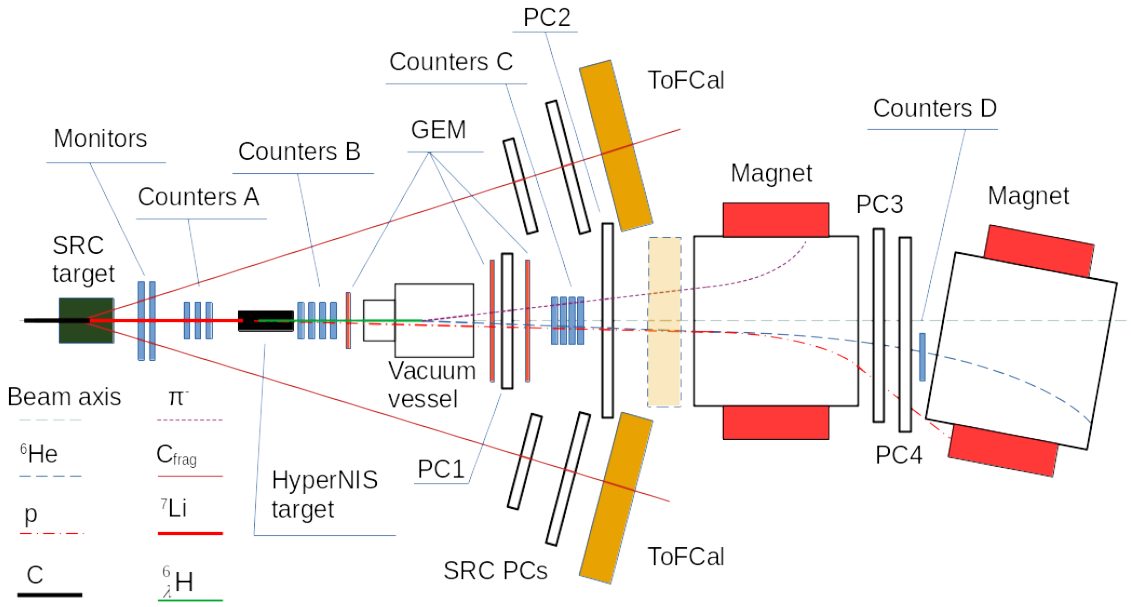

Figure 5: The configuration of the HyperNIS+SRC spectrometer is presented in particular, for the search of ${}^{6}_{\Lambda}$H hypernuclei with the ^{7}Li beam (not in scale). The scheme contains: the HyperNIS target; beam monitor counters; groups of trigger counters A, B, and C; the vacuum decay vessel of 55 cm length; 4 groups of proportional chambers PC1–PC4; the ToFCal station which should be installed in front of the first magnet (the faded rectangular on the scheme); two analyzing magnets with the magnetic field 0.6T (only one is used for this configuration); the scintillation counter D which confirms the registration of ^{6}He nuclei, i.e., detects that a daughter nucleus is not ^{3}H but ^{6}He. The HyperNIS carbon target has sizes $12 \times 3 \times 3$ cm and the density 20.4 g/cm^2.

of proportional chambers PC1 (four chambers 38×38 cm^2) and PC2 (two chambers 130×80 cm^2) register hits from pion and the daughter He nucleus, allowing the reconstruction of the decay vertex. In addition, the set of all the proportional chambers, PC1–PC4, is used to measure the momentum of the He nucleus. The chambers PC3 and PC4 are of the same size as the chambers PC2. The full set of the chambers allows to detect the secondary proton or another ^{7}Li fragment and to separate the momentum of the daughter nucleus produced in the decay of the hydrogen hypernucleus, i.e., a helium isotope. The scintillation counters D are used to measure and to record the signal amplitude to separate ^{6}He daughter nuclei from tritium fragments produced together with ${}^{4}_{\Lambda}$H hypernuclei.

4 Experimental method

We would like to underline six main features of the method elaborated at JINR:

1. It is based on the idea to investigate a high energy hypernucleus produced due to a beam nucleus excitation.

2. Such hypernucleus decays occur outside the target that allows one to organize a selective trigger and to identify produced isotopes separating daughter nucleus momenta.

3. The trigger is tuned to find pionic decays of hypernuclei when the charge of the daughter nucleus is higher than that of the hypernucleus and no physical event can simulate the such charge (and, consequently, the counter signal) relation.

4. Decay products are forwardly collimated. Therefore, the spectrometer acceptance is high.

5. We analyze events when the hypernucleus decay vertex is observed in vacuum where no background interaction can simulate the decay.

6. Momenta of different hypernucleus isotopes are separated by large gaps (like momenta of daughter nuclei which are measured by the spectrometer) and therefore, it is easy to identify isotopes ^{3}He, ^{4}He, and ^{6}He.

In Fig. 6 we present calculated ^{3}He, ^{4}He, and ^{6}He momentum distributions for the reaction

$$^7\mathrm{Li} + \mathrm{C} \rightarrow {}^A_\Lambda\mathrm{H} + \mathrm{p(d,t,n)} + \ldots \rightarrow {}^A\mathrm{He} + \pi^- + \mathrm{p(d,t,n)} + \ldots, \quad A = 3, 4, 6.$$

Fig. 7 shows that even in the case of large possible errors of momentum measurements,

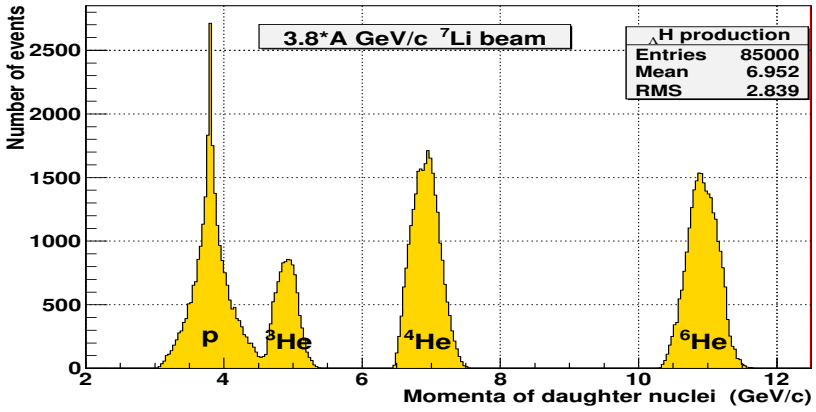

Figure 6: The expected distribution of daughter helium momentum divided by their charge. Helium is the product of hydrogen hypernucleus decay. The proton peak is the calculated momenta of protons produced in Li fragmentation when ${}^6_\Lambda$H is produced. The peaks can be easy separated in order to identify different produced hyperhydrogen isotopes.

for example, 2%, peaks are clearly separated.

In order to measure momenta of relatively slow pions emitted at quite large angles, the time-of-flight method will be used. For this purpose, ToFCal walls should be moved to the magnet entrance so that due to the 12 cm wide gap they do not distort helium momenta. The ToF system will be used to determine masses of hypernuclei.

Also it should be taken into account that the decay vertices can be found safely if the decay opening angle is not too narrow. We estimate the efficiency of vertex reconstruction at a level of 90% since opening angles are concentrated at higher values, see Fig. 11. In calculations presented in Figs. 6 and 7, the minimal distance between

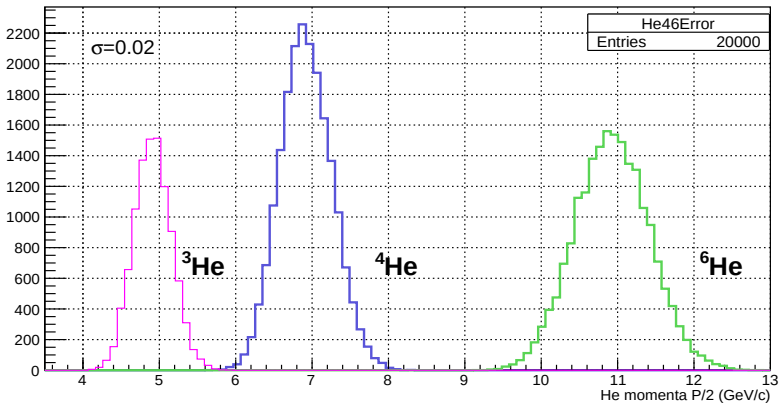

Figure 7: The expected distribution of daughter helium momentum divided by their charge in the case of 2% momentum error distribution. If ${}^{6}_{\Lambda}$H are produced, ${}^{4}_{\Lambda}$H and ${}^{6}_{\Lambda}$H peaks can be easily separated.

He and pion hits in the proportional chambers was chosen equal to 3 cm to be sure that the decay vertex position can be reconstructed. However, this cut should be proved experimentally with high statistics of events when two particles leave a thin target.

In 2022 two GEM detectors of 40 × 40 cm size were produced at CERN. They can reduce the number of events rejected due to the narrow opening angle (see below) and to increase the accuracy of location of the hypernucleus decay point. As a result, the tracking efficiency will be improved as well. Monte-Carlo (MC) calculations have been performed to choose optimal geometry of the target and proportional chambers. We should remind that decay products, i.e. pions and daughter nuclei, are forward collimated so that we can find chamber positions to register more than 90% of decay pions. Certainly, all daughter nuclei hit proportional chambers.

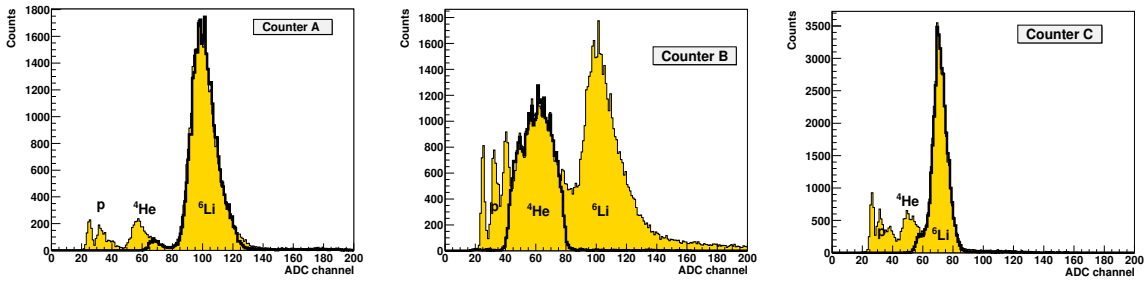

Figure 8: Tuning of trigger (scintillation) counters with the ^{6}Li beam for ${}^{6}_{\Lambda}$He production and the decay. Examples of spectra of the signal amplitude obtained for counters A, B, and C, correspondingly, are shown. Peaks of the signal amplitude correspond to the lithium beam and its fragments from interactions with the Al target inserted into the beam to produce different lithium fragments i.e., helium and hydrogen isotopes. The part of spectrum discriminated by thick line contours, is determined by counter discriminators which are tuned to register lithium for counters A and C and helium for the counters B. As it was mentioned, scintillation counters B were replaced with Cherenkov counters.

A trigger was developed for detection of pionic decays of hypernuclei. It was used successfully in the previous experiment in Dubna [5, 6, 18]. The idea of the trigger is as follows. When the ${}^{6}_{\Lambda}$H hypernucleus is produced, the ^{7}Li nucleus has to emit a

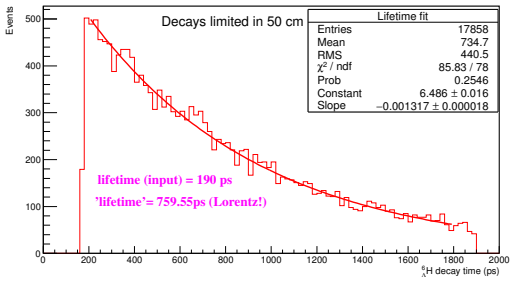

Figure 9: The expected decay time distribution inside of the 50 cm distance is shown. Due to the Lorentz factor, the distribution is exponential with the decay parameter equal to 760 ps in the case of the 190 ps lifetime.

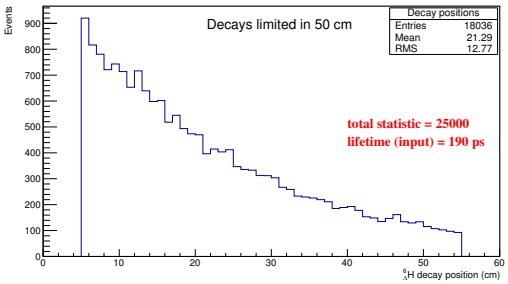

Figure 10: Expected decay points inside of the 50 cm decay volume are plotted. Since 25000 events were analyzed and about 18000 decays of hypernuclei were found inside of the 50 cm distance, we obtain the probability of approximately 70% that the first point is at the distance of 5 cm from the target.

spectator proton while the remaining core, the ^{6}He nucleus, is transmuted into $^6_\Lambda$H. Each of these two particles has the charge equal to 1 (total $Z = 1 + 1$) and hits the block of the Cherenkov counters B. Since the counter response is proportional to Z^2 of the interacting particle, both particles will create in the Cherenkov counters B signals proportional to the sum of charge squares, $U = 1^2 + 1^2 = 2$. As performed MC calculations show, less than 2-3% of recoil protons or slow associated K^+ hit Cherenkov counters B which are insensitive to slow particles.

The mesonic decay $^6_\Lambda$H$\rightarrow^6$He$+\pi^-$ produces particles with $Z = 2$ (He) and $Z = -1$ (π^-). The scintillation counters C of a minimal size are used in order to register mainly the daughter helium nuclei. Most pions will miss these counters and such the condition provides the best amplitude resolution of counters C. It is also expected that a significant fraction of the spectator protons will hit the counters. However, it is desirable to have a trigger working at the full capacity and therefore, one should ensure that the trigger works efficiently when the counters C have a signal proportional to $U = 2^2 = 4$ for the case when only helium hits the counters C, $U = 2^2 + 1^2 = 5$ when proton or pion also hit the counters, and $U = 2^2 + 1^2 + 1^2 = 6$ when all particles hit. So, the counters C should produce a signal proportional to $U \geq 4$ *if a hydrogen hypernucleus decay takes place* but less than $U = 9$ created by Li beam nuclei. Finally, let us underline that for the case of pionic decays, the signal registered in the counters C is higher than one obtained in the set B while for majority of background events the situation is opposite. Counters SciHe, see Fig. 5, are not a part of the trigger. Their signals are recorded and are used to check that helium-6 registered in chambers PC3 and PC4 is not background tritium. Some results of trigger tests were presented in [41, 42].

As was noted above, a significant part of hypernuclei decays straight off after the target. For example, if we assume the lifetime of the $^6_\Lambda$H hypernucleus equal to 190 ps, then the ^{7}Li beam with the momentum[1] 27 GeV/c produces hypernuclei with the lifetime at the laboratory frame about 760 ps due to the Lorentz factor, see Fig. 9. As

[1]The highest value available at the beam line is 3.8 GeV/c per nucleon.

shown in Fig. 10, the mentioned physical effect provides a possibility to expect 70% of hypernuclei decays inside of our vacuum vessel if it is placed at the distance of 5 cm from the target.

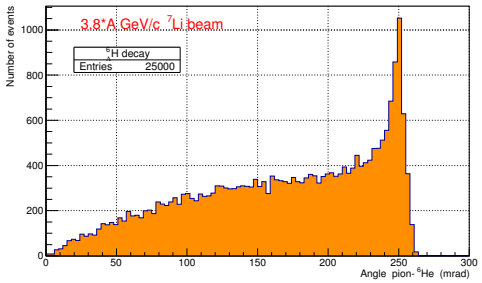

Figure 11: The distribution of the calculated pion helium separation angle for ${}^{6}_{\Lambda}\mathrm{H} \rightarrow \pi^{-} + {}^{6}\mathrm{He}$ decays is shown. About 10-16% decays have separation angles below resolution of the proportional chambers but can be detected using GEM detectors in future experiments.

In order to optimize the efficiency, one should check if the short distance between the target and the vacuumed decay volume does not cause additional losses due to a narrow angle between momenta of pion and helium which is the hypernucleus daughter nucleus. Estimates show that the possible shortest distance between the target and the decay volume is the best choice. By increasing this distance we loose statistics not only due to early decays but also for the reason that pions miss the acceptance of the proportional chambers while losses due to a narrow separation angle stay in 10-16% interval and therefore, are less significant. The distribution of the He-π separation angle for the case of ${}^{6}_{\Lambda}\mathrm{H}$ decays is presented in Fig. 11. Some results of the calculated pion distribution at proportional chambers are shown in Figs. 12 and 13.

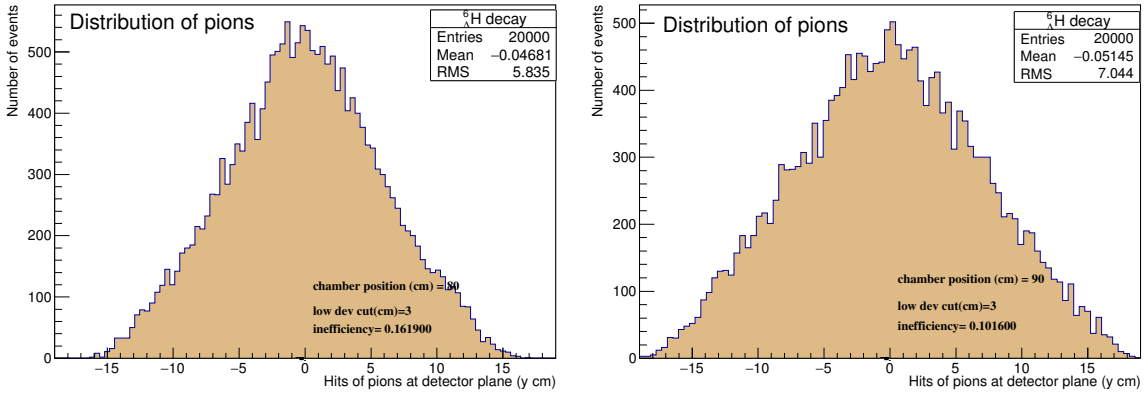

Figure 12: We demonstrate the distribution of pion hits in a proportional chamber situated at distances 80 cm (left panel) or 90 cm (right panel) from the beam entrance point of the target. There are no decay pions outside the chamber. For example, an arbitrary quite large value of the minimal distance between He and pion hits is chosen equal to 3 cm as a limit of inefficiency. The cut in the real experiment will be optimized.

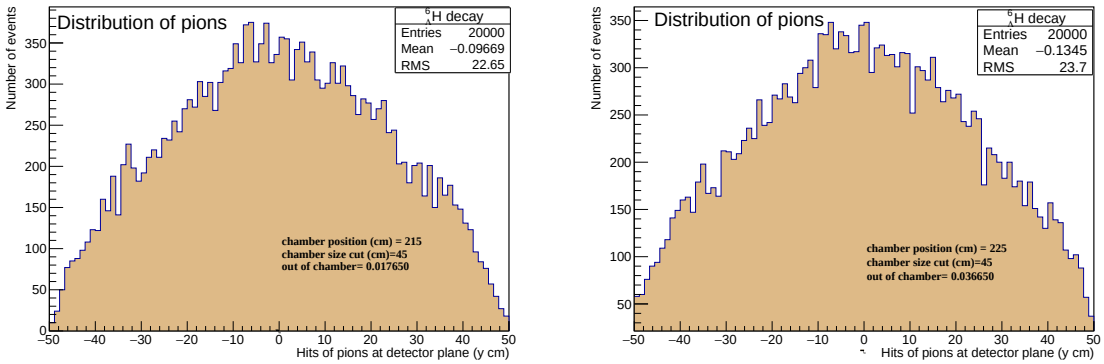

Figure 13: Pion hits at the last chamber which pions traverse, are shown. The geometrical efficiency depends the shift of the target position. The shift on 10 cm results in few percent loss as we see confronting left and right panels. For the experiment, the distance of 215 cm is chosen.

5 Results obtained in the last years

During the Nuclotron run 50 the ^{7}Li beam was delivered to the spectrometer for the first time. The provided beam time was used mostly for tests and tuning of the modernized trigger system in the new counting room located at the new place in the experimental hall. The background suppression factor much higher than 10^4, was reached.

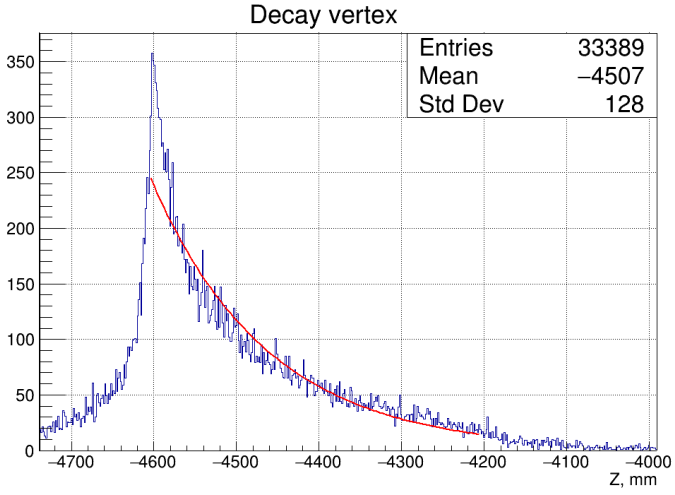

Figure 14: Properly reconstructed decay points allow one to measure the lifetime of a hypernucleus. The left edge of the fiducial decay volume is at $Z = -4600$ mm.

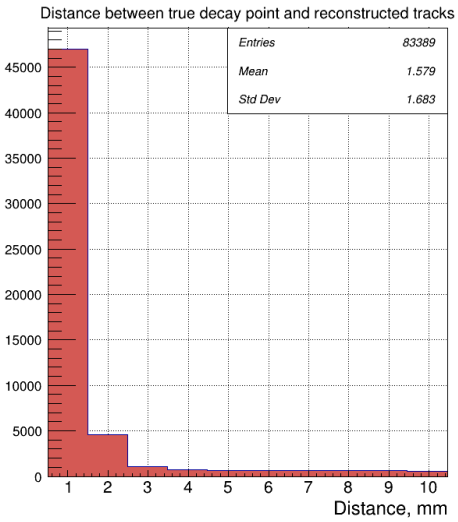

Figure 15: Decay points can be localized into 2 mm.

Recently the tracking software was upgraded and became more effective. Some results of tests with MC generated events are presented in Figs. 14 and 15.

In the last years the Nuclotron upgrade was a task of highest priority for the laboratory. We were waiting when the energy of the extracted nuclear beam will exceed the hypernucleus production threshold on such the value which allows to carry

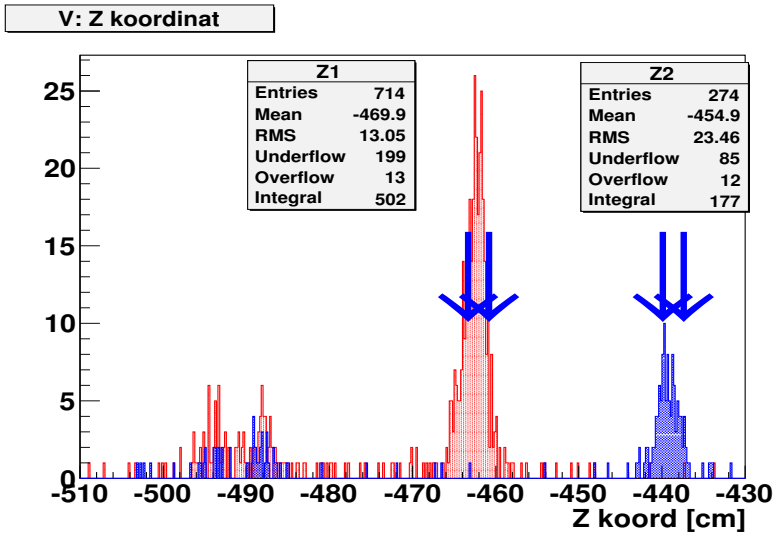

Figure 16: Positions of reconstructed ${}^{6}_{\Lambda}$H along the beam axis are plotted. The results of a test of alignment codes and vertex reconstruction procedure are presented. The target was placed at two positions (red and blue histograms). The arrows show the edges of the target. The position of two monitor trigger counters is also seen. The vertex position is the point of the minimal distance between two tracks ($d < 2$ mm).

out hypernuclear experiments. During this time the deuteron beam was used for short test runs in order to calibrate the spectrometer and to test the new equipment. Data for alignment of proportional chambers were taken, few software applications for alignment were developed and investigated, and all necessary calculations and fits were performed. Some results are presented in Fig. 16.

At the present time the kinetic energy of the extracted nuclear beam is increased up to $4A$ GeV that is essentially higher than the hypernucleus production threshold. Also the beam line to the HyperNIS spectrometer was tested and the necessary nuclear beam was transported to the spectrometer. Unfortunately, in 2017-2022 the Li beam was available only for a short (63 hours) test run which was used to tune the trigger for hypernucleus detection and to test chambers. The duration of this run was too short for data taking.

On the other hand, the spectrometer was significantly upgraded during the last years. For example, a new electronic gas supply system allows one to stabilize the performance of proportional chambers.

But the most important improvement was taken place in R&D and production of new front-end electronics for proportional chambers. Two hundreds analog signal cards with 32 inputs in each card were produced in Minsk. The digital part of the FEE cards, see Figs. 17 and 18, was designed and tested in JINR.

Electronic modules of the trigger system were replaced with new ones too. All modules in VME crate, i.e., time charge digital converter (TQDC), data acquisition (DAQ), and service modules, and the main DAQ server are new. It should be underline that a new universal amplitude digitizer, DT5560S 32 Ch. 14 bit 125 MS/s, was bought and software tests was started. The usage of DT5560S allows us to remove the large amount of cable connections and provides a possibility to write signal amplitudes and

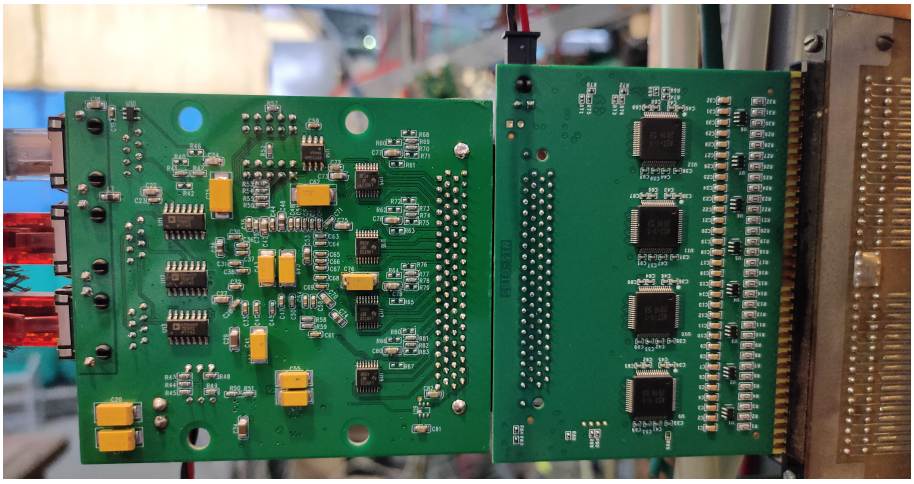

Figure 17: The FEE cards are shown. The left plate is the digital part for data processing and transfer. The right plate is the the analog signal amplifier part where one can see chamber output contacts.

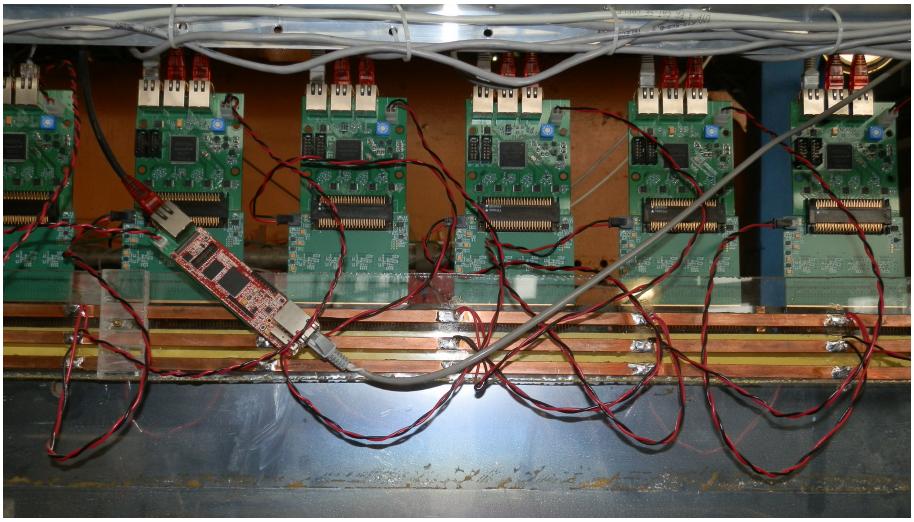

Figure 18: FEE cards on a proportional chamber are shown.

times of all counters of the trigger system. As a result, we will make thresholds of the preliminary hardware trigger softer to use the digital final software trigger later and to select hypernuclear events more carefully. Systems of on-line service as the beam control, monitoring of the chamber efficiencies, the slow control for high voltage supply units, and others, were elaborated, tested, and are used. Since the beam intensity in the hypernuclear experiments is relatively low, $10^5 - 10^6 s^{-1}$, it is necessary to organize the Internet access to the beam control data for the Nuclotron staff. Moreover, taking into account experience of test runs, this system is upgraded from run to run. All data from trigger counters are available in the Nuclotron control room and can be used by the staff to improve beam tuning.

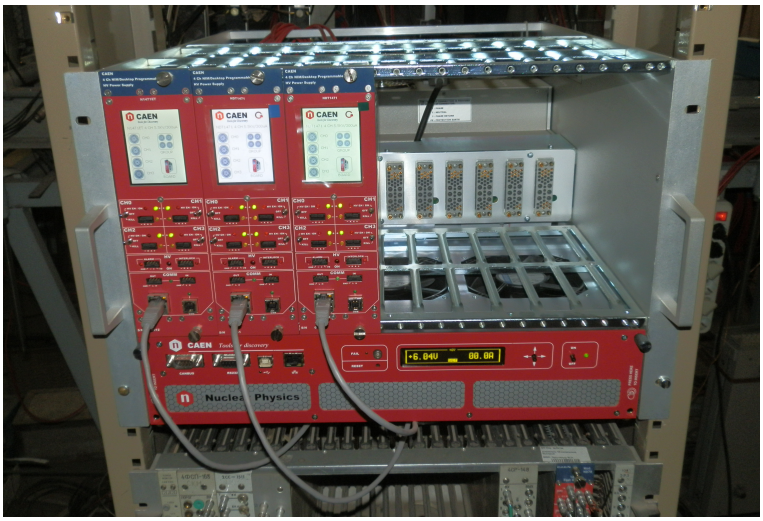

Figure 19: The NIM crate with the CAEN high voltage power supply for proportional chambers is shown.

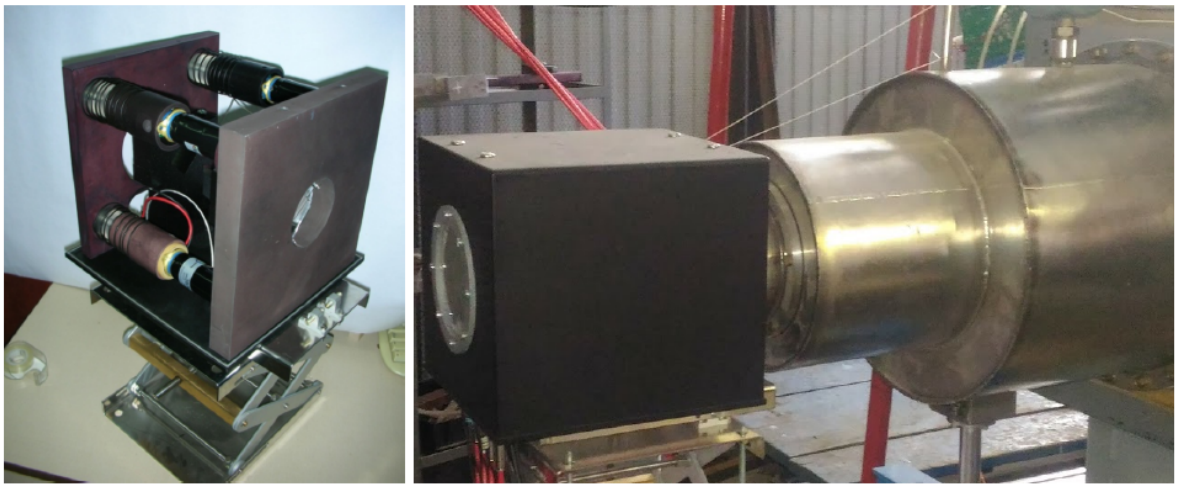

Figure 20: The block of four Cherenkov counters with four subsequent quartz radiators each of the 4 mm thick, is demonstrated. On the left side, one can see three of four Electron Tubes 9107B photomultipliers. The high density graphite (1.7 g/cm^3) target is placed closely to radiators. The block itself is placed near the vacuum vessel as you can see on the right side of the figure.

A new high voltage supply system was put into operation for trigger photomultiplier tubes. It has up to 64 very stable outputs driven by WIENER MPOD crate controller. The corresponding programs was adapted by HyperNIS members. The proportional chambers are driven using CAEN high voltage supply modules, see Fig. 19. In time, low voltage systems for proportional chambers were obtained and installed as well. Recently, a block of four Cherenkov trigger counters was produced. The carbon target is situated inside of the block closely to quartz radiators in order to minimize losses of observed hypernuclei due to decays[2]. The produced Cherenkov block was tested and the amplitude resolution was obtained higher than in the caseof the scintillation

[2]Approximately 20% of hypernuclei decay at very first five centimeters after the target.

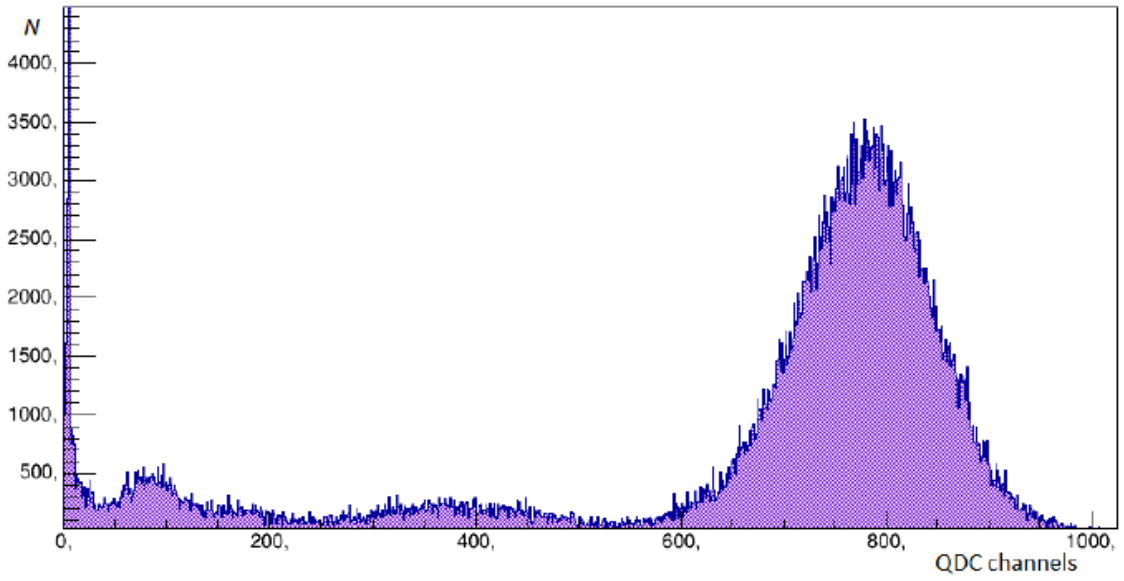

Figure 21: The pulse height distribution of lithium fragments measured with one of the Cherenkov counters. A clean separation is obtained for hydrogen, helium, and lithium.

counter block, see Figs. 20 and 21.

To reject the possible background of nuclear fragments produced in the trigger counters, primarily tritium, several additional scintillation counters (the set D) were produced and tested.

6 Plan for the coming years

Taking into account that two different experiments are proposed, first one with the ^{7}Li beam and the second with the carbon beam, one should carefully plan the change of beams and tasks. For the hypernuclear experiment, the optimal schedule can be like that below:

- The focus will be made on the hypernuclear program of the HyperNIS project with the use of the d and ^{7}Li beams (the deuteron beam is needed for methodical purposes). In 2023-2024 two GEM detectors will be installed to improve the decay vertex localization.

- The study of the hypernucleus ${}^{6}_{\Lambda}$H in 2023-2024: the search of ${}^{6}_{\Lambda}$H with subsequent measurements of the lifetime with the accuracy of $10-15$ ps, the production cross section, and the mass with accuracy of $1-2$ MeV if the isotope exists. Minimal necessary statistics for these goals is about 500 detected events of ${}^{6}_{\Lambda}$H production. If the production cross section is as low as in the case of ${}^{3}_{\Lambda}$H, approximately two hundred hours of the lithium beam are necessary.

If the first ${}^{6}_{\Lambda}$H experiment is successful, we will continue to take 2000 detected events of ${}^{6}_{\Lambda}$H production to check predictions of two lifetimes of ${}^{6}_{\Lambda}$H isomeric states or to search for the ${}^{8}_{\Lambda}$H hypernucleus using the ^{9}Li beam. The last task is preferable.

- In 2023-2024 the technical design and mounting which are necessary for SRC detectors and the additional magnet, will be performed.

- In 2025 the study of poorly investigated ${}^{6}_{\Lambda}$He has to be made including measurements of the lifetime and the production cross section. At least 500 events of ${}^{6}_{\Lambda}$He production have to be detected.

- In 2025-2026 we are planning the search of ${}^{8}_{\Lambda}$H hypernucleus, the study of non-mesonic decay of medium hypernuclei ${}^{10}_{\Lambda}$Be and ${}^{10}_{\Lambda}$B, and tests for the measurement of Coulomb dissociation of ${}^{3}_{\Lambda}$H which requires high statistics due to rare events of production and decay of hypernuclei ${}^{10}_{\Lambda}$Be and ${}^{10}_{\Lambda}$B. Fortunately, this task can be simultaneously solved with the data collection for the SRC experiment.

The first stage of the research program of the HyperNIS project has to be finished in 2026. The most important technical result of the project is that a new multipurpose magnetic spectrometer with modern detectors and electronics will be commissioned and will be ready for hypernuclear experiments using extracted Nuclotron beams. The spectrometer will be also available for other experiments, e.g., tests of detectors and so on.

7 Present status of the apparatus.

After test runs at the Nuclotron beam, the HyperNIS spectrometer is commissioned. The extracted beams of deuteron, ^{6}Li, and ^{7}Li with the kinetic energy of $1.0 - 3.5$ GeV/nucleon and the intensity of $10^4 - 10^5$ s^{-1} were used in the test runs.

To provide particles with different electric charges for the trigger tests, the ^{6}Li beam passed through the aluminium target. The composition of the resulted beam after the target is shown in Fig. 8. Similarly, the resolution of the counters and that the counter response is directly proportional to the ionization were tested with the carbon beam, see an example of the signal amplitude spectrum for carbon and its fragments in Fig. 22.

It should be noted again that trigger electronics was upgraded in the last few years. Any possibility to have a beam, was used to test the trigger for the study of hypernuclei even if the beam was not suitable for hypernuclear experiments. While early tests give the background suppression of the order of $2.5 \cdot 10^3$, see, for example, [42], the background rejection of the order of 10^4 was achieved in the test run with the ^{7}Li beam. We would like to underline that we use two triggers simultaneously. One of them is aimed to search for production and decays of hypernuclei while the second is included to check that the spectrometer performance is good. Since the rate of the hypernucleus

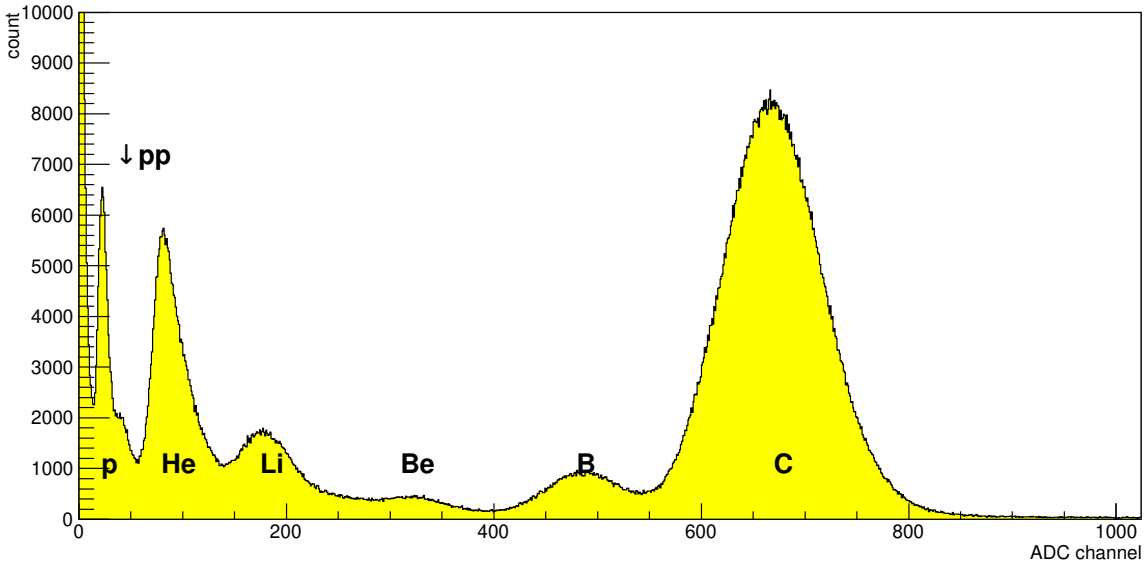

Figure 22: Amplitudes of carbon fragments measured for the carbon beam at the Al target are shown for a trigger scintillation counter.

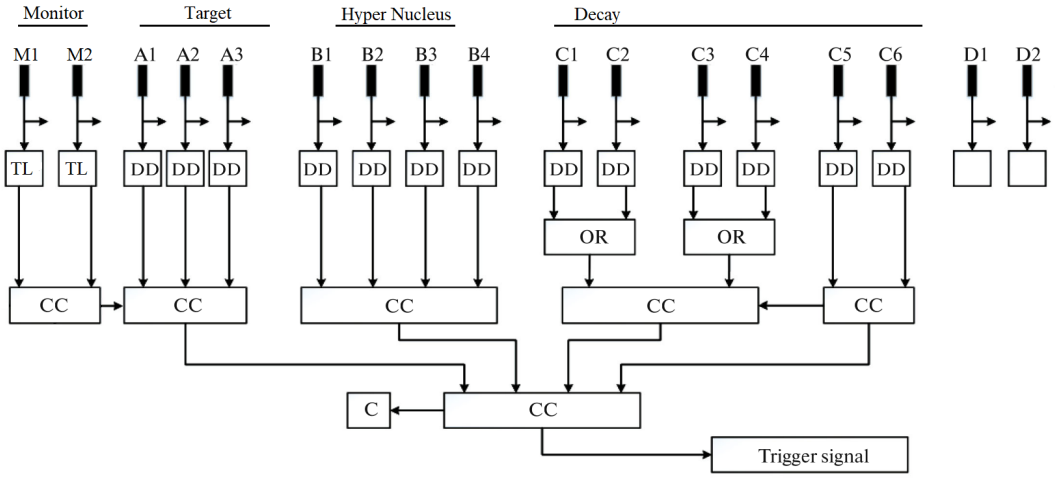

Figure 23: Schematic of reception of the trigger signal: (filled rectangles) PEMs, (DD) differential discriminators, (TL) time locking scheme, (OR) logical adders, (CC) coincidence circuits, and (C) counting circuit.

trigger is low, the second trigger was tuned to detect events every 100 ms when a minimum ionizing particle (MIP) particle crosses counters and proportional chambers. This trigger is used for checking efficiency of all chambers and for the on-line control in the analysis of systematic errors.

The hypernucleus trigger shown in Fig. 23, must select events with the following signature:

- "good" incoming beam particles hitting the target are detected, i.e., particles with the charge $Z_{mon} = 3$ for which no other particles appear during approximately

30 ns before and after the hit [43]. This selection is realized by coincidence of signals of the "monitor" and "target" trigger parts;

- after the target but before the decay region, a particle with the charge $Z = Z_{mon} - 1$ is detected with help of the "hypernucleus" section;
- after the decay region, a particle with the charge $Z = Z_{mon}$ is detected with help of the "decay" section.

If the such sequential change of the charge, $U = 3 \to U = 2 \to 4 \leq U < 9$, is found, the trigger generates the signal as shown in Fig. 23 for the reaction

$$^{7}\mathrm{Li} + \mathrm{C} \to {}^{A}_{\Lambda}\mathrm{H} + \mathrm{p(d,t,n)} + \ldots \to {}^{A}\mathrm{He} + \pi^{-} + \mathrm{p(d,t,n)} + \ldots, \quad A = 3, 4, 6.$$

A test run was carried out with the renovated trigger system situated in the new counting room and for the ^{7}Li beam with the high energy, $3A$ GeV. This run showed that the trigger can be tuned to suppress the background by a factor much higher than 10^4 [43]. The production of GEM detectors was completed but they have not been delivered to Dubna yet due to logistical difficulties. An advantage of the GEM is that readout electronics is similar to one used at LHEP experiments and can be integrated into our DAQ system. This detector improves the algorithm for the search of a hypernucleus decay vertex. If GEM is installed between the trigger block B and vacuum and registers three particles, we reject the event because all tree particles are emitted from the target and do not originate from a decay in vacuum. Further, in 2021 it was proposed to install two modern GEMs produced at CERN, at the HyperNIS spectrometer. These detectors, GEM1 and GEM2, will have dimensions of the active area 400×400 mm and the distance 0.5 mm between strips. We are going to install GEM1 before the first block of proportional chambers and GEM2 behind it. The space resolution of both GEMs will be near 400 μm which allows to increase the angular accuracy for tracks in two times. Furthermore, using these detectors will enlarge useful statistics by 10% since nearly 15% of events contain tracks within a narrow cone and can not be distinguished in the first MWPC. Inclusion of GEMs also results in that localization of decay vertices and, consequently, the accuracy of lifetime measurements will be improved.

8 Conclusions

The study of properties of lightest hypernuclei is relevant, has high importance, and can be performed at JINR with beams from Nuclotron. The trigger of the HyperNIS spectrometer works with a high suppression factor and efficiency. Installing and commissioning of the new FEE allow us to significantly improve tracking efficiency and to carry out the proposed hypernuclear experiments. It can give answers to open questions in hypernuclear physics which are very hard for answering by alternative methods and approaches. At present time the HyperNIS spectrometer is tested using beta sources and cosmic muons.

It should be noted that the HyperNIS spectrometer and the beam line can easily be used to test detectors. HyperNIS test runs were used (and can be used in future) to test pixel detectors (TimePix) from IEAP, Prague, microstrip detectors for a satellite experiment, etc. TimePix tests were carried out together with Prague's team. These tests provided good experience for young Czech researchers. Also several students for JINR were trained. An upgrade of the spectrometer, tuning of new modules and counters, and test runs have shown that the HyperNIS team is ready to achieve stated aims.

References

[1] M. Agnello *et al.* (FINUDA Collaboration), Phys. Rev. Lett. **108**, 042501 (2012).

[2] E. Botta, Nucl. Phys. A **914**, 119 (2013).

[3] M. Agnello *et al.*, Nucl. Phys. A **881**, 269 (2012).

[4] H. Sugimura *et al.* (J-PARC E10 Collaboration), Phys. Lett. B **729**, 39 (2014).

[5] A. U. Abdurakhimov *et al.*, Nuovo Cim. A **102**, 645 (1989).

[6] S. Avramenko *et al.*, Nucl. Phys. A **547**, 95 (1992).

[7] H. Bandō *et al.*, Nucl. Phys. A **501**, 900 (1989).

[8] H. Bandō, T. Motoba, and J. Žofka , Int. J. Mod. Phys. A **5**, 4021 (1990).

[9] Y. Xu, JPS Conf. Proc. **17**, 021005 (2017).

[10] S. Piano, JPS Conf. Proc. **17**, 021004 (2017).

[11] C. Rappold and T. Saito, JPS Conf. Proc. **17**, 021003 (2017).

[12] H. Kamada *et al.*, Phys. Rev. C **57**, 1595 (1998).

[13] T. Motoba *et al.*, Nucl. Phys. A **534**, 597 (1991).

[14] B. Donigus, AIP Conf. Proc. **2130**, 020017 (2019).

[15] L. Adamczyk *et al.* (STAR Collaboration), Phys. Rev. C **97**, 054909 (2018).

[16] ALICE Collaboration, arXiv: 2209.07360 [nucl-ex].

[17] M. S. Abdallah *et al.* (STAR Collaboration), arXiv: 2110.09513 [nucl-ex].

[18] Yu. A. Batusov *et al.*, Phys. Part. Nucl. **36**, 169 (2005) [Fiz. Elem. Chast. Atom. Yadra **36**, 319 (2005)].

[19] T. R. Saito *et al.*, *Proc. of the IX International Conference on Hypernuclear and Strange Particle Physics (HYP06), 2006, Mainz*, ed. by J. Pochodzalla and Th. Walcher, Springer, Berlin, Heidelberg (2007), 171.

[20] C. Rappold *et al.*, Nucl.Phys. A **913**, 170 (2013).

[21] S. A. Avramenko *et al.*, Nucl. Phys. A **585**, 91 (1995).

[22] Z. Arzoumanian *et al.*, Astrophys. J. Suppl. **235**, 37 (2018); J. Antoniadis *et al.*, Science **340**, 1233232 (2013); H. T. Cromartie *et al.*, Nature Astronomy **4**, 72 (2019).

[23] D. Logoteta, I. Vidana, and I. Bombaci, Eur. Phys. J. A **55**, 207 (2019) [arXiv: 1906.11722].

[24] A. Sakaguchi, JPS Conf. Proc. **17**, 011007 (2017).

[25] T. Nagae, Nucl. Phys. A **914**, 559 (2013).

[26] E. Hiyama *et al.*, Nucl. Phys. A **908**, 29 (2013).

[27] A. Gal and D.J. Millener, Phys. Lett. B **725**, 445 (2013) [arXiv: 1305.6716].

[28] B. F. Gibson and I. R. Afnan, Nucl. Phys. A **914**, 179 (2013); Few-Body Systems **55**, 913 (2014).

[29] L. Majling, Nucl. Phys. A **585**, 211 (1995).

[30] L. Majling, *Proc. of the IX International Conference on Hypernuclear and Strange Particle Physics (HYP06), 2006, Mainz*, ed. by J. Pochodzalla and Th. Walcher, Springer, Berlin, Heidelberg (2007), 149.

[31] R. H. Dalitz and R. Levi Setti, Nuovo Cimento **30**, 489 (1963).

[32] Y. Akaishi and T. Yamazaki, Frascati Phys. Ser. **16**, 59 (1999).

[33] K. S. Myint and Y. Akaishi, Progr. Theor. Phys. Suppl. **146**, 599 (2003).

[34] S. Shinmura *et al.*, J. Phys. G **28**, L1 (2002).

[35] S. A. Avramenko *et al.*, JINR Communication P1-91-206, Dubna (1991).

[36] J. Lukstins, Nucl. Phys. A **691**, 491 (2001).

[37] S. V. Afanasiev *et al.*, *Proc. of the IX International Conference on Hypernuclear and Strange Particle Physics (HYP06), 2006, Mainz*, ed. by J. Pochodzalla and Th. Walcher, Springer, Berlin, Heidelberg (2007), 165.

[38] M. V. Evlanov *et al.*, Nucl. Phys. A **632**, 624 (1998); Part. Nucl. Lett. **105**, 5 (2001).

[39] L. Majling and Yu. Batusov, Nucl. Phys. A **691**, 185c (2001).

[40] M. M. Block and R. H. Dalitz, Phys. Rev. Lett. **11**, 96 (1963).

[41] R. A. Salmin, O. V. Borodina, A. I. Maksimchuk, and V. L.Rapatsky, The talk at the LHE JINR Seminar on relativistic nuclear physics, June 06, 2007.

[42] V. D. Aksinenko *et al.*, *Proc. of XIX International Baldin Seminar on High Energy Physics Problems "Relativistic Nuclear Physics and Quantum Chromodynamics", Dubna, September 29 - October 4, 2008)*, JINR, Dubna, 2008, 155.

[43] A. V. Averyanov *et al.*, Phys. Part. Nuclei Lett. **16**, 826 (2019).